

Doubly differential cross sections of secondary electrons ejected from molecular oxygen by electron impact

T. W. Shyn and W. E. Sharp

Space Physics Research Laboratory, University of Michigan, Ann Arbor, Michigan 48109

(Received 24 September 1990)

A measurement of the doubly differential cross sections of secondary electrons ejected from molecular oxygen by electron impact has been made. A modulated crossed-beam method was used with incident electron energies from 25 to 250 eV. The energy and angular range of secondary electrons covered from 1.0 eV to one-half of the difference between the incident energy and ionization potential and from 12° to 156° , respectively. The present results have been compared with the previous measurements and considerable discrepancies were found.

I. INTRODUCTION

Molecular oxygen is an abundant gas in the earth's atmosphere where it is bombarded by ultraviolet solar photons and energetic electrons. Thus, it is useful to study the interaction of O_2 with electrons in order to examine the paths through which these electrons are losing their energy. There have been a number of measurements of the total ionization cross section. Tate and Smith,¹ Asundi *et al.*,² and Rapp and Englander-Golden³ have measured total ionization cross sections of O_2 by electron impact and their results are consistent with each other. In order to understand the physical processes in the collision, the cross sections as a function of angle and ejected secondary-electron energy is the meaningful quantity. The only measurement of this doubly differentially cross sections (DDCS) on O_2 has been made by Opal, Beaty and Peterson.⁴ These measurements were restricted to the secondary-electron energy and angular range 4-eV to one-half of the incident energy and 30° to 150° , respectively. Incident energies between 50 and 2000 eV were used. The important energy region below 4 eV for secondary electrons were not measured. This region is where a large fraction of the ionization cross section originates.

This paper presents results of experiments in which the DDCS of secondary electrons ejected from O_2 have been measured by electron impact over a wider angular range than previously done. Secondary-electron energies below 4 eV are also measured. Discrepancies between the DDCS of the present results and those of Opal, Beaty, and Peterson are evident, particularly at the lower energies and extreme angles.

II. APPARATUS AND PROCEDURE

The apparatus used for the present measurements is the same as that used previously for He (Ref. 5), N_2 (Ref. 6), and H_2 (Ref. 7). A brief description is given here. Differentially pumped upper and lower chambers contain the apparatus. A neutral molecular oxygen beam source is in the upper chamber. The vertically collimated neutral beam from the source is modulated by a chopper and

enters the lower chamber through a double skimmer located between the two chambers. The monoenergetic electron beam source and an electron energy analyzer system (in a horizontal plane) are located in the lower chamber. The electron beam source consists of an electron gun, a 127° energy sector, two electron lenses, and two electron beam deflectors. It is rotatable from -90° to $+160^\circ$ continuously. During the present set of measurements, the electron source produces an electron current of 10^{-7} A with an energy resolution of 150 meV [full width at half maximum (FWHM)], approximately. The divergence angle of the beam is $\pm 3^\circ$. The fixed detector system located also in the lower chamber consists of an electrostatic energy analyzer (127°), two electron lenses, and a channeltron electron multiplier.

The incident electron beam of a given energy in the horizontal plane intersects with the vertically collimated neutral beam in an interaction region. The ejected electrons from the beam at a given angle are detected by the electron channeltron multiplier after energy analysis. The final results have been placed on an absolute scale using the elastic cross sections of O_2 at each incident energy measured by Shyn and Sharp.⁸

Three sets of helmholtz coils reduce stray magnetic fields down to less than 20 mG in all directions near the interaction region.

III. EXPERIMENTAL RESULTS

The DDCS of secondary electrons have been measured at the incident energies of 25, 50, 75, 100, 150, and 250 eV by utilizing a modulated crossed-beam method. The measured energy and angular range of secondary electrons were from 1.0 eV to the half of the difference between the incident energy and ionization potential, and from 12° to 156° , respectively.

The results of DDCS are given in Tables I–VI. Singly differential cross section (SDCS) obtained by integrating DDCS over solid angles are also given in Tables I–VI as the last column. The total ionization cross sections deduced from these data along with other measurements are shown in Table VII.

The statistical uncertainty of the data points is less

TABLE I. DDCCS (10^{-19} cm²/eV sr) at 25-eV impact. Numbers in parentheses are extrapolated data points.

θ (deg)	12	24	36	48	60	72	84	96	108	120	132	144	156	168	$\Delta\sigma/\Delta E$ (10^{-18} cm ² /eV)
1.0	55.3	24.6	13.0	6.2	3.9	2.3	2.3	2.5	3.0	3.4	4.1	4.3	4.3	(4.3)	7.6
2.0	38.9	18.2	13.2	8.2	5.3	3.8	3.8	4.0	4.3	5.7	6.0	6.4	7.3	(7.7)	8.8
3.0	34.0	16.1	12.1	9.8	5.3	3.9	3.8	4.1	4.4	5.5	6.1	6.9	7.0	(7.3)	8.9
4.0	30.8	15.2	12.3	9.0	5.2	4.1	4.0	4.1	4.5	5.1	5.7	6.6	6.7	(6.8)	8.5
5.0	22.3	14.4	11.0	8.6	4.9	4.1	3.8	3.9	4.2	4.7	5.3	6.2	6.5	(6.8)	7.8
6.5	21.2	13.7	8.9	6.8	4.3	3.9	3.7	3.5	3.4	3.8	4.4	5.1	6.0	(7.0)	6.8

TABLE II. DDCCS (10^{-19} cm²/eV sr) at 50-eV impact. Numbers in parentheses are extrapolated data points.

θ (deg)	12	24	36	48	60	72	84	96	108	120	132	144	156	168	$\Delta\sigma/\Delta E$ (10^{-18} cm ² /eV)
1.0	66.2	39.7	24.5	7.6	6.7	4.4	4.6	3.9	4.8	5.4	8.5	10.2	13.4	(18.9)	13.1
2.0	52.9	35.3	27.2	14.4	7.3	6.9	7.3	7.8	9.4	10.7	12.4	12.7	13.1	(14.0)	16.2
3.0	44.1	32.3	22.9	18.2	11.2	8.9	9.2	10.1	10.9	13.6	14.6	14.9	15.6	(16.2)	18.2
4.0	36.8	27.8	20.0	14.1	9.2	7.9	7.6	8.6	9.3	10.1	11.3	12.3	12.9	(13.5)	15.0
5.0	36.8	25.3	18.8	12.6	9.5	7.4	7.3	7.3	7.9	8.2	9.3	10.3	10.7	(10.9)	13.4
6.0	20.6	14.6	10.2	9.6	7.7	6.3	6.2	6.2	6.2	6.8	7.8	8.3	8.5	(8.8)	10.1
8.0	17.6	14.1	11.3	9.0	6.9	5.7	5.5	5.5	5.6	6.5	7.1	8.0	9.0	(10.3)	9.6
10.0	21.9	14.3	10.9	8.4	6.7	5.8	5.3	5.3	5.5	5.9	6.5	7.6	8.2	(8.5)	9.3
12	21.0	14.5	10.9	8.3	6.6	5.4	5.1	4.9	5.2	5.6	6.1	7.1	7.9	(8.8)	8.8
15	19.7	12.3	8.4	6.8	6.0	4.6	4.3	4.0	4.2	4.7	5.3	6.5	7.2	(8.1)	7.5
19	26.3	14.3	9.0	6.6	5.1	4.3	3.7	3.4	3.5	4.1	5.2	6.5	8.2	(10.3)	7.5

TABLE III. DDCCS (10^{-19} cm²/eV sr) at 75-eV impact. Numbers in parentheses are extrapolated data points.

θ (deg)	12	24	36	48	60	72	84	96	108	120	132	144	156	168	$\Delta\sigma/\Delta E$ (10^{-18} cm ² /eV)
1.0	99.8	54.4	28.2	13.6	7.1	6.8	6.2	7.3	8.1	9.0	11.4	13.0	16.7	(20.6)	18.4
2.0	68.6	44.1	29.5	18.9	11.0	9.8	10.0	16.3	12.2	15.6	17.3	17.6	16.3	(16.7)	21.5
3.0	49.8	32.7	23.1	14.5	10.9	10.2	10.8	11.6	12.3	14.5	16.6	17.9	16.2	(15.4)	19.4
4.0	44.4	31.2	20.4	13.9	10.4	9.1	9.0	9.5	10.4	12.1	13.8	14.9	14.4	(14.5)	17.0
5.0	33.5	21.4	14.4	11.7	8.1	7.6	7.8	7.8	8.5	9.8	10.8	12.0	12.9	(14.4)	13.5
6.0	28.7	20.6	15.3	11.7	8.5	6.7	6.7	7.0	7.2	7.9	8.7	9.7	10.6	(11.7)	12.3
8.0	24.1	14.3	10.0	8.1	6.3	5.7	5.5	5.5	5.7	6.2	6.9	7.7	8.4	(9.4)	9.3
10	15.1	10.1	7.9	7.2	6.2	5.7	5.6	5.4	5.5	6.0	6.5	7.4	8.3	(9.3)	8.4
12	12.2	9.3	7.3	6.5	5.9	5.4	5.0	4.9	5.1	5.4	6.0	6.9	7.8	(8.7)	7.7
15	13.0	8.4	7.1	6.6	5.0	4.4	4.1	3.9	4.0	4.4	5.2	5.9	6.9	(8.0)	6.6
20	11.5	7.7	5.8	5.0	4.4	3.6	3.2	3.1	3.1	3.2	4.2	5.1	6.0	(7.0)	5.5
25	11.7	7.7	5.3	4.4	3.5	3.0	2.6	2.4	2.4	2.8	3.6	4.4	5.5	(6.8)	4.8
31.4	17.9	9.9	5.6	4.2	3.4	2.5	2.1	1.9	2.0	2.5	3.2	4.4	5.7	(7.3)	4.8

TABLE IV. DDCCS (10^{-19} cm²/eV sr) at 100-eV impact. Numbers in parentheses are extrapolated data points.

θ (deg)	12	24	36	48	60	72	84	96	108	120	132	144	156	168	$\Delta\sigma/\Delta E$ (10^{-18} cm ² /eV)
1.0	67.2	37.0	20.5	10.7	6.6	4.9	5.6	5.4	5.8	6.9	8.4	8.8	9.9	(11.8)	13.1
2.0	55.4	39.0	28.0	17.2	10.1	8.1	8.2	8.8	9.7	11.9	12.7	13.7	14.8	(17.0)	18.1
3.0	40.3	32.4	21.9	15.3	10.0	9.2	9.7	10.2	11.1	13.5	15.3	16.5	15.9	(15.7)	18.0
4.0	34.5	27.7	19.4	12.9	10.2	8.4	8.5	8.8	9.7	12.0	12.1	13.1	12.7	(12.6)	15.5
5.0	27.0	20.8	14.7	10.7	7.6	6.9	7.1	7.3	7.7	8.6	9.5	10.1	9.8	(9.5)	12.1
6.0	24.0	18.5	12.9	9.7	7.2	6.6	6.5	6.6	7.9	8.1	8.1	8.6	9.0	(9.4)	11.0
8.0	19.9	12.2	10.5	7.4	6.4	5.6	5.4	5.3	5.5	5.8	6.1	6.5	7.1	(7.8)	8.6
10	15.5	8.8	7.3	6.7	5.9	5.2	4.9	5.1	5.2	5.6	6.0	6.8	7.7	(8.8)	7.8
12	14.0	9.2	8.1	6.5	5.6	5.1	4.8	4.6	4.6	4.8	5.3	5.9	6.5	(7.2)	7.3
15	11.4	8.5	6.9	5.8	5.1	4.5	4.4	4.0	4.2	4.4	4.9	5.4	7.2	(7.4)	6.6
20	7.4	5.5	4.5	4.0	3.6	3.2	2.9	2.7	2.7	2.8	3.2	3.7	4.4	(5.1)	4.4
25	6.4	4.7	3.9	3.5	3.0	2.5	2.3	2.0	2.1	2.3	2.6	3.1	3.6	(4.3)	3.6
30	6.1	4.1	3.5	3.0	2.4	2.0	1.7	1.6	1.6	1.8	2.1	2.5	3.0	(3.6)	3.0
35	6.7	4.5	3.2	2.8	2.3	1.6	1.4	1.3	1.3	1.5	1.9	2.4	3.0	(3.8)	2.7
40	8.8	5.3	3.4	2.7	2.1	1.5	1.2	1.2	1.1	1.4	1.7	2.3	2.8	(3.5)	2.7
43.9	10.9	6.0	3.4	2.7	1.9	1.3	1.1	0.9	1.1	1.2	1.7	2.3	2.8	(3.6)	2.7

TABLE V. DDCS (10^{-19} cm²/eV sr) at 150-eV impact. Numbers in parentheses are extrapolated data points.

E_s (eV) \ θ (deg)	12	24	36	48	60	72	84	96	108	120	132	144	156	168	$\Delta\sigma/\Delta E$ (10^{-18} cm ² /eV)
1.0	50.2	29.9	19.4	10.2	6.3	4.6	4.8	4.6	5.3	6.7	7.1	7.4	8.5	(9.8)	11.4
2.0	75.0	38.9	27.1	16.0	11.2	8.8	9.2	9.7	10.5	11.4	12.3	12.8	13.8	(15.4)	18.6
3.0	56.5	25.2	17.0	13.4	10.9	10.2	10.2	10.6	11.0	11.6	12.2	11.8	11.7	(11.5)	16.6
4.0	49.4	30.1	21.2	14.2	11.6	9.5	9.5	9.7	10.5	10.8	11.4	10.9	10.9	(11.2)	16.4
5.0	38.5	20.0	14.9	10.5	9.1	8.1	8.1	8.0	8.2	8.6	8.8	8.4	8.7	(9.2)	12.7
6.0	31.3	17.3	13.2	10.6	8.3	7.4	7.4	7.3	7.4	7.7	7.9	7.7	7.6	(7.6)	11.4
8.0	20.5	10.9	9.6	7.3	6.1	5.6	5.5	5.4	5.5	5.5	5.8	5.9	6.0	(6.1)	8.3
10	15.2	10.0	8.5	6.4	5.4	5.0	4.9	4.8	4.9	5.1	5.3	5.5	5.9	(6.2)	7.4
12	10.1	7.3	6.5	5.5	4.6	4.6	4.4	4.2	4.3	4.4	4.9	5.4	5.6	(5.9)	6.3
15	8.8	6.2	5.3	4.9	4.1	3.9	3.7	3.5	3.5	3.6	3.8	4.2	4.6	(5.0)	5.3
20	6.6	4.6	4.3	4.0	3.5	3.1	2.8	2.6	2.5	2.5	2.8	3.0	3.3	(3.5)	4.0
25	4.8	3.5	3.2	3.2	2.7	2.3	2.1	1.9	1.8	1.8	1.9	2.1	2.3	(2.6)	3.0
30	3.3	2.4	2.3	2.3	2.0	1.7	1.4	1.3	1.2	1.3	1.3	1.5	1.8	(2.2)	2.1
35	2.9	2.3	2.0	2.0	1.7	1.4	1.2	1.2	1.1	1.1	1.2	1.3	1.6	(2.1)	1.8
40	2.7	2.0	1.6	1.4	1.2	0.9	0.8	0.7	0.7	0.7	0.8	1.0	1.2	(1.4)	1.3
50	2.7	1.8	1.4	1.2	0.9	0.7	0.6	0.5	0.5	0.5	0.6	0.8	0.9	(1.1)	1.0
60	3.4	2.1	1.4	1.1	0.8	0.5	0.4	0.4	0.4	0.5	0.5	0.7	0.9	(1.1)	0.96
69	4.7	2.8	1.5	1.2	0.8	0.5	0.4	0.3	0.3	0.4	0.5	0.7	0.8	(1.1)	1.0

TABLE VI. DDCS (10^{-19} cm²/eV sr) at 250-eV impact. Numbers in parentheses are extrapolated data points.

E_s (eV) \ θ (deg)	12	24	36	48	60	72	84	96	108	120	132	144	156	168	$\Delta\sigma/\Delta E$ (10^{-18} cm ² /eV)
1.0	90.9	21.8	12.4	6.1	3.8	3.6	3.1	3.3	3.6	4.2	4.5	4.5	4.6	(4.8)	9.0
2.0	48.0	29.6	20.2	15.4	8.7	7.5	7.6	7.7	7.7	8.8	9.8	10.5	11.8	(11.9)	14.7
3.0	48.0	23.9	20.2	12.8	8.5	8.4	8.7	9.2	10.1	10.6	10.6	10.7	10.7	(10.9)	15.0
4.0	44.0	27.0	21.3	12.8	10.6	8.9	9.0	9.0	9.4	10.1	10.4	10.5	10.8	(11.1)	15.3
5.0	41.6	20.5	16.7	11.1	8.1	7.9	7.9	7.7	8.1	8.1	8.6	8.4	8.4	(8.4)	12.6
6.0	29.3	18.4	15.1	10.0	7.6	6.6	6.5	6.8	6.7	6.8	7.0	7.4	7.4	(7.4)	10.8
8.0	21.1	9.9	8.0	6.7	5.3	5.2	5.1	4.9	5.0	5.1	5.3	5.3	5.4	(5.6)	7.5
10	14.3	9.1	7.5	5.7	5.2	5.0	4.7	4.5	4.6	4.6	4.8	4.7	4.7	(4.7)	6.7
12	12.0	7.2	6.4	5.6	4.5	4.3	4.0	3.9	3.9	3.9	4.0	4.4	4.6	(4.8)	5.9
15	9.4	6.1	5.4	4.9	4.2	3.9	3.6	3.4	3.3	3.2	3.4	3.5	3.6	(3.8)	5.0
20	5.5	3.9	3.6	3.5	3.0	2.8	2.6	2.5	2.2	2.2	2.3	2.4	2.6	(2.8)	3.5
25	3.9	2.9	2.8	3.0	2.5	2.4	2.1	1.8	1.7	1.6	1.7	1.8	1.9	(2.1)	2.7
30	3.2	2.3	2.2	2.4	1.9	1.8	1.5	1.3	1.2	1.2	1.2	1.3	1.5	(1.6)	2.1
35	2.6	2.0	1.8	1.9	1.7	1.5	1.2	1.1	1.1	1.0	0.9	1.0	1.1	(1.3)	1.7
40	1.7	1.4	1.4	1.5	1.3	1.1	0.92	0.77	0.71	0.71	0.72	0.8	0.92	(1.1)	1.3
50	1.3	0.97	0.92	1.06	0.92	0.76	0.62	0.50	0.42	0.43	0.47	0.53	0.61	(0.70)	0.85
65	0.97	0.74	0.70	0.78	0.55	0.46	0.33	0.28	0.26	0.26	0.29	0.33	0.37	(0.49)	0.55
80	0.98	0.70	0.60	0.63	0.45	0.32	0.21	0.18	0.17	0.17	0.19	0.25	0.26	(0.28)	0.42
100	1.2	0.78	0.60	0.51	0.31	0.19	0.14	0.12	0.11	0.12	0.14	0.16	0.22	(0.30)	0.34
118.7	1.5	0.96	0.64	0.42	0.25	0.17	0.11	0.09	0.09	0.10	0.12	0.14	0.18	(0.23)	0.32

TABLE VII. Total ionization cross sections (10^{-16} cm²).

E_i (eV)	Present results	Ref. 4	Ref. 3	Ref. 1	Ref. 2
15			0.85		0.88
20			0.31	0.35	0.40
25	0.56				
30			0.90	1.06	1.1
50	1.96	1.91	1.88	2.46	2.2
75	2.54				
80			2.51	2.64	2.56
100	2.58	2.89	2.67	2.74	
150	2.68		2.69	2.81	
200		2.75	2.53	2.64	
250	2.41		2.36	2.46	
300		2.06	2.18	2.20	

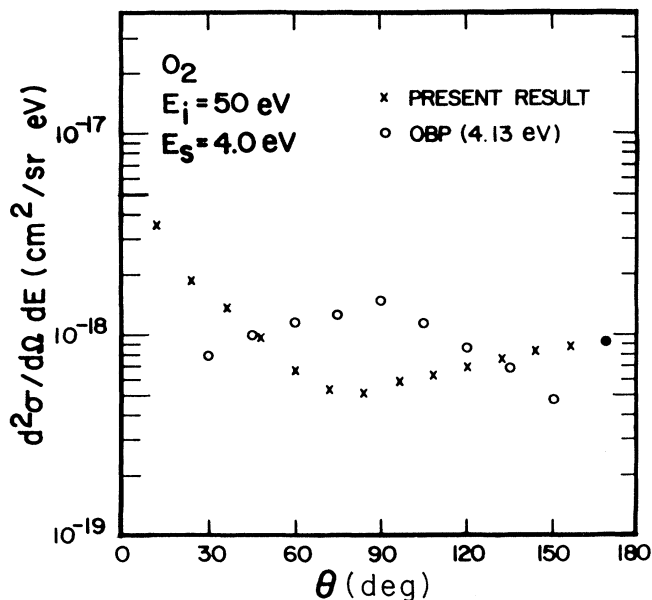


FIG. 1. DDCC at 4.0-eV secondary electrons ejected from O_2 at 50-eV electron impact along with those of Opal, Beaty, and Peterson (at 4.13 eV). Solid dot is an extrapolated data point.

than 4%. The uncertainty in the normalization process is less than 10%. Including the uncertainty in elastic cross sections ($\pm 14\%$), the resultant uncertainty of the present results is $\pm 18\%$.

Figure 1 shows the DDCC of 4.0-eV secondary electrons at 50-eV electron impact energy along with the result of Opal, Beaty, and Peterson at 4.13-eV secondary-electron energy. The angular distribution of Opal, Beaty, and Peterson has the opposite shape of the present results as well as a larger value at 90° than the present result by a factor of 2. The shape of Opal, Beaty, and Peterson may be a result of an overcorrection on the volume effects at extreme angles in their experiments.

Figure 2 shows the DDCC of 40-eV secondary electron

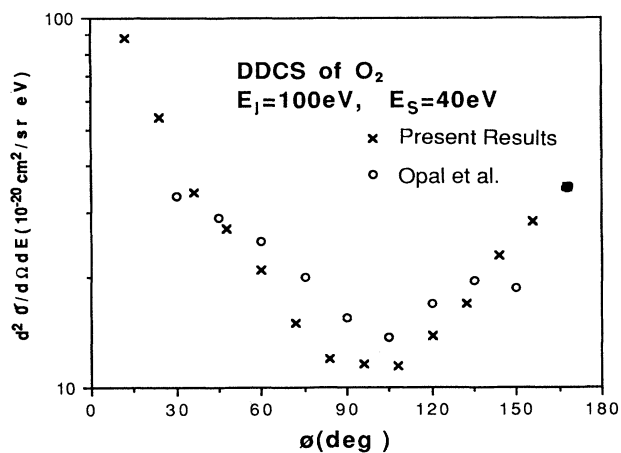


FIG. 2. DDCC of 40-eV secondary electrons ejected from O_2 at 100-eV electron impact along with those of Opal, Beaty, and Peterson. Solid dot is an extrapolated data point.

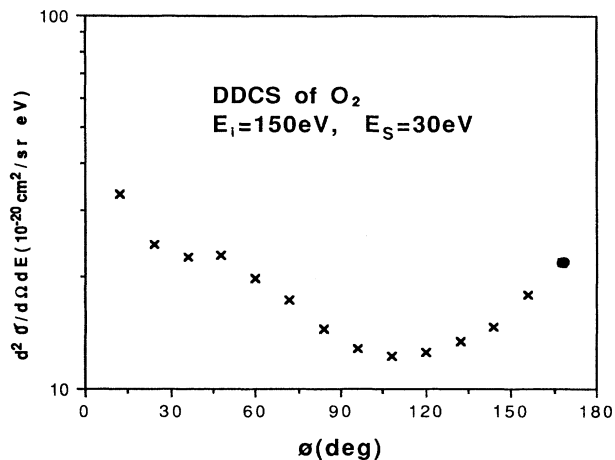


FIG. 3. DDCC of 30-eV secondary electrons ejected from O_2 at 150-eV electron impact. Solid dot is an extrapolated data point.

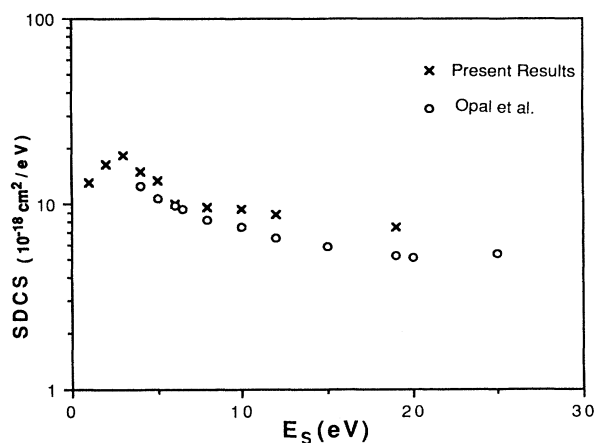


FIG. 4. SDCS of O_2 at 50-eV electron impact along with those of Opal, Beaty, and Peterson.

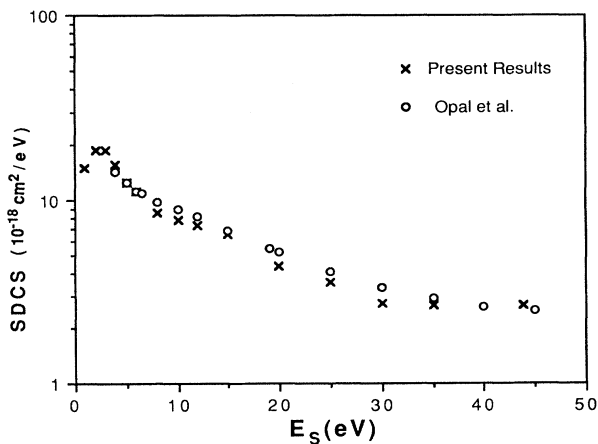


FIG. 5. SDCS of O_2 at 100-eV electron impact along with those of Opal, Beaty, and Peterson.

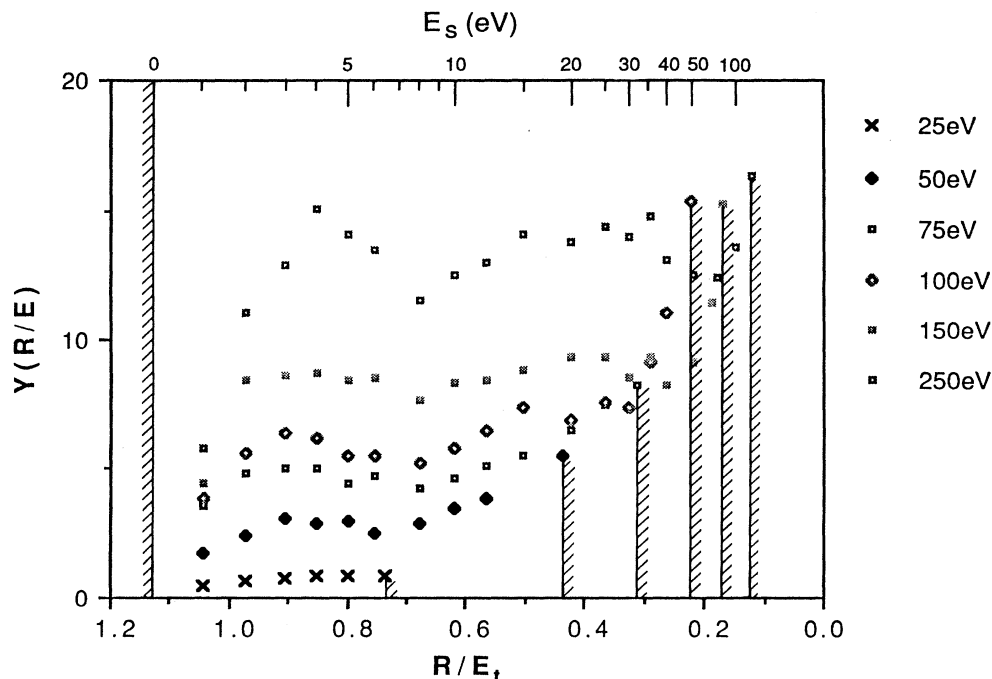


FIG. 6. Platzman plot at 25-, 50-, 75-, 100-, 150-, and 250-eV electron impact on O_2 .

energy at 100-eV impact energy along with those of Opal, Beatty, and Peterson. At the extreme angles, there is a disagreement. This may be for the same reason mentioned in Fig. 1. Also the magnitude of our DDCS at 90° is lower by 25%.

Figure 3 shows the DDCS of 30-eV secondary electrons at 150-eV impact. There is a minimum near 105° and relatively strong forward and backward scatterings. The small peak near 60° is the "binary peak" due to the conservation of momentum and energy in the colliding system.

Singly differential cross sections at 50-eV electron impact are shown in Fig. 4 along with those of Opal, Beatty, and Peterson. The present results extend much lower energies and are generally larger by approximately 25% than those of Opal, Beatty, and Peterson. There is a maximum of SDCS at 3.0 eV secondary electron energy.

Figure 5 shows the SDCS at 100-eV impact energy. For higher energies there is agreement between our measurements and those of Opal, Beatty, and Peterson even though the DDCS are considerably different from each other. There is a maximum of SDCS near 2.0-eV secondary electron energy.

Figure 6 shows the Platzman plot of the present results. A detailed description about the Platzman plot can be found in Ref. 7. Briefly, the ordinate, $Y(R/E_s)$, is the ratio of SDCS and the Rutherford cross section [$d\sigma/dE_s = (4\pi a_0^2/E_i)(R/E_i)^2$, where E_i is the incident energy and E_i is the sum of the ionization potential and the secondary electron energy E_s , a_0 is the Bohr radius, and R is the Rydberg energy] and the abscissa is R/E_i . The secondary-electron energy scale is added on the top of the plot. The Platzman plot shows the sum of the dipole-allowed and the nondipole part (Mott cross sec-

tion). At high incident energy where the Born approximation is valid, the dipole-allowed part of the Platzman plot resembles the photoionization cross section. Also the plot amplifies the region of low secondary electrons where the major contributions to total ionization cross section come from and the area under the plot is directly proportional to the total ionization cross section. The Platzman plot of the present results shows two maxima near 4- and 30-eV secondary-electron energies and the peaks are more visible as the incident energy increases. Also it is noted that all the values of $Y(R/E)$ decrease as the secondary-electron energy decreases. The Platzman

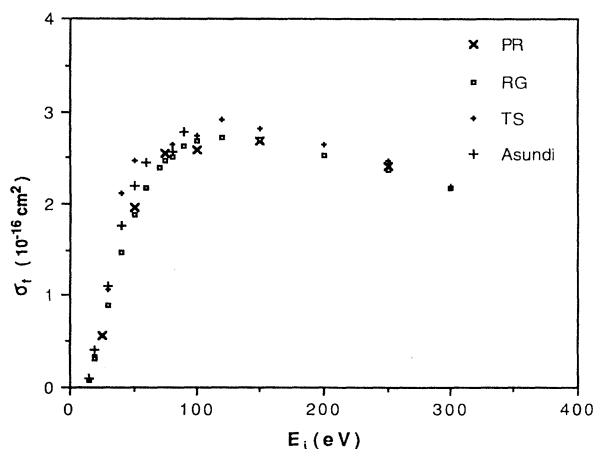


FIG. 7. Total ionization cross section of O_2 by electron impact [present results (PR)] along with those of Rapp and Golden-Glander (RG), Take and Smith (TS), and Asundi.

plot resembles more the photoionization cross sections measured by Samson, Rayborn, and Pareek⁹ (Fig. 3 in their paper) as the incident energy increases. However, it seems that the incident energy 250 eV does not reach the region where the Born approximation is valid. A broad maximum near 30-eV secondary-electron energy may come from the dissociative ionization and the autoionization of oxygen molecules may contribute the other maximum near 4-eV secondary-electron energy.

All of the SDCS at given incident energies were integrated over the secondary-electron energy to give the total ionization cross section. These results are shown in Fig. 7 along with those of Opal, Beaty, and Peterson, Rapp and Englander-Golden, Tate and Smith, and those

of Asundi, Craggs, and Kurepa. There is very good agreement between the present results and those of Rapp and Englander-Golden, and those of Opal, Beaty, and Peterson. However, those of Tate and Smith are generally higher than the present results by about 20% below 100 eV. The results of Asundi, Craggs, and Kurepa are systematically higher than the present results by about 10%. It should be noted that the present results include multi-ionization cross sections (double and triple, etc.).

ACKNOWLEDGMENTS

This work was supported by National Science Foundation Grant No. ATM-8913022.

¹J. T. Tate and P. T. Smith, *Phys. Rev.* **39**, 270 (1932).

²R. K. Asundi, J. D. Craggs, and M. V. Kurepa, *Proc. Phys. Soc. (London)* **82**, 967 (1963).

³D. Rapp, and P. Englander-Golden, *J. Chem. Phys.* **43**, 1464 (1965).

⁴C. B. Opal, E. C. Beaty, and W. K. Peterson, *At. Data* **4**, 209 (1972).

⁵T. W. Shyn and W. E. Sharp, *Phys. Rev. A* **19**, 557 (1979).

⁶T. W. Shyn, *Phys. Rev. A* **27**, 2388 (1983).

⁷T. W. Shyn, W. E. Sharp, and Y.-K. Kim, *Phys. Rev. A* **24**, 79 (1981).

⁸T. W. Shyn and W. E. Sharp, *Phys. Rev. A* **26**, 1369 (1982).

⁹J. A. R. Samson, G. H. Rayborn, and P. N. Pareek, *J. Chem. Phys.* **76**, 393 (1982).